

Statistical and dynamical fluctuations of Binder ratios in heavy ion collisions

Zhiming Li, Fengbo Xiong, and Yuanfang Wu

*Institute of Particle Physics, Central China Normal University, Wuhan 430079, China
Key Laboratory of Quark and Lepton Physics (Central China Normal University), Ministry of Education*

Higher moments of net-proton Binder ratio, which is suggested to be a good observation to locate the QCD critical point, is measured in relativistic heavy ion collisions. We firstly estimate the effect of statistical fluctuations of the third and forth order Binder ratios. Then the dynamical Binder ratio is proposed and investigated in both transport and statistical models. The energy dependence of dynamical Binder ratios with different system sizes at RHIC beam scan energies are presented and discussed.

PACS numbers: 25.75.Gz, 25.75.Nq

I. INTRODUCTION

One of the main goals of current relativistic heavy ion collisions is to map the QCD phase diagram [1]. At vanishing baryon chemical potential $\mu_B = 0$, finite temperature Lattice QCD calculations predict that a cross-over transition from hadronic phase to the Quark Gluon Plasma (QGP) phase will occur around a temperature of 170 - 190 MeV [2, 3]. QCD based model calculations indicate that the transition could be a first order at large μ_B [4]. The point where the first order phase transition ends is the so-called QCD Critical Point (QCP) [5, 6]. Attempts are being made to locate the QCP both experimentally and theoretically [7]. Lattice QCD calculations at finite μ_B face numerical challenges in computing. Thus the location of the QCP are highly uncertain in theoretically. In experimental aspect, the RHIC beam energy scan program [8] has been motivated to search for the QCP in experiment. By decreasing the collision energy down to a center of mass of 5 GeV, RHIC will be able to vary the baryon potential from $\mu_B \sim 0$ to 500 MeV.

Fluctuations of conserved charges, which behave differently between the hadronic and QGP phase, are generally considered to be sensitive indicators for the transition [9, 10]. The singularity at the QCP, at which the transition is believed to be second order, may cause enhancement of fluctuations if fireballs created by heavy ion collisions pass near the critical point during the time evolution [11]. It has been shown that near the critical point, the density-density correlator of baryon number follow the same power law behavior as the correlator of the sigma field which is associated with the chiral order parameter [11, 12]. Therefore, the baryon number is considered as an equivalent order parameter of formed system in nuclear collisions. In experiment, net-proton multiplicity distribution is much easier to measure than the net-baryon numbers. Theoretical calculations have shown that in QCD with exact isospin invariance, the relevant corrections due to isospin breaking are small and the net-proton fluctuations can reflect the singularity of the baryon number susceptibility as expected at the QCP [13]. Hence, the net-proton number is used in

current heavy ion experiment [14].

It is suggested recently that the Binder-like ratios are good identification of critical behavior in relativistic heavy ion collisions[15–17]. The third and forth order Binder ratios are defined as

$$\begin{aligned} B_3 &= \frac{\langle M^3 \rangle}{\langle M^2 \rangle^{3/2}} \\ B_4 &= \frac{\langle M^4 \rangle}{\langle M^2 \rangle^2}, \end{aligned} \quad (1)$$

where M can be a conserved net-charge, e.g. the net-baryon number. The Binder ratio is a new observable in heavy ion collisions. The difference between Binder ratios and the well-known higher moments[14, 18] is that Binder ratios are the normalized higher raw moments while the higher moments are central moments.

The universality argument indicates that the static critical exponents of the second order phase transition are determined by the dimensionality and symmetry of the system. The QCD critical point of deconfinement phase transition belongs to the same universality class as liquid-gas phase transition and the 3D-Ising model [11, 12, 19]. Its universal critical properties are discussed to be valid in various of models and relevant to heavy ion collisions [11, 20, 21], in particular the event-by-event fluctuations of baryon numbers [11].

In the calculations of the 3D-Ising model[15] with external field $h = 0$, Binder ratios of B_3 and B_4 as a function of temperature (T) show a step jump from a lower platform to a higher one near the vicinity of critical point. If we could map the parameters (T, h) of the Ising model onto the parameters (T, μ) along the freeze-out curve in QCD and find a path that correspond to $h = 0$, the critical behaviors of 3D-Ising model is expected for the QCD critical point. Therefore, if the formed system in heavy ion collisions reaches the critical point and the freeze-out curve is close to the transition line, the step function liked behavior of Binder ratios in the Ising model may serve as a probe of QCP in current heavy ion collisions, where critical incident energy is difficult to assign precisely in priori.

In the mean time, the effect of trivial statistical fluctuations [22] due to insufficient number of particles should

be studied and properly eliminated in higher moment calculations. Therefore, we should discuss the statistical contributions from the measured fluctuations firstly, then we could identify the dynamical part which is more relevant to the critical point of the QCD phase transition.

In this paper, we firstly investigate the statistical and dynamical fluctuations of net-proton Binder ratios by using the AMPT and THERMINATOR models. Then, the energy dependence of dynamical Binder ratios in Au + Au collisions at various RHIC beam scan energies are studied.

In our analysis, two versions of a multi-phase transport (AMPT) model [23] are used. One is the AMPT default and the other one is the AMPT with string melting. In both versions, the initial conditions are obtained from the heavy ion jet interaction generator (HIJING) model, and then the scattering among partons is given by the Zhangs parton cascade (ZPC) model. In the AMPT default model, the partons recombine with their parent strings when they stop interacting, and the resulting strings are converted to hadrons using the Lund string fragmentation model, whereas in the AMPT model with string melting, quark coalescence is used in combining partons into hadrons. The dynamics of the hadronic matter is described by the ART model. The THERMINATOR statistical model [24] is a Monte Carlo event generator designed for studying of particle production in relativistic heavy ion collisions from SPS to LHC energies. It implements thermal models of particle production with single freeze out.

In order to make our calculations convenient for comparison with the RHIC beam energy scan data, we choose the mid-rapidity ($|y| < 0.5$) region with transverse momentum $0.4 < p_T < 0.8$ GeV/c. This phase space is where the STAR experiment can do the particle identification for proton numbers with its main tracking detector - the Time Projection Chamber [14]. The number of events used in this analysis is around 6 million. This statistics is needed for the calculation of the dynamical Binder ratios of net-proton to ensure the statistical errors under control.

II. STATISTICAL FLUCTUATIONS OF BINDER RATIOS

In the measurement of the net-proton Binder ratios, finite number of protons and antiprotons will cause non-negligible statistical fluctuations. If the produced protons and antiprotons are two independent Poisson-like distributions [22, 25], the net-protons then obey a Skellam (SK) distribution [26].

According to the definition of Eq. (1), the statistical fluctuations of the net-proton Binder ratios can be directly deduced from the Skellam distribution

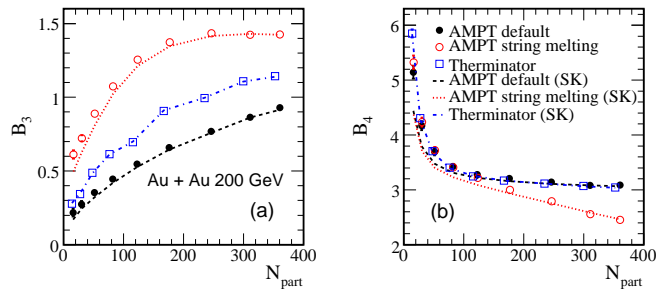


FIG. 1: Binder ratios of B_3 (a) and B_4 (b) as a function of number of participants from AMPT default (solid circle), AMPT with string melting (open circle), and THERMINATOR (open square) models in Au + Au collisions at $\sqrt{s_{NN}} = 200$ GeV. The dashed lines represent the corresponding statistical fluctuations.

$$B_{3,stat} = \frac{\Delta^3 + 6\mu\Delta + \Delta}{(\Delta^2 + 2\mu)^{3/2}}$$

$$B_{4,stat} = \frac{\Delta^4 + 12\mu\Delta^2 + 4\Delta^2 + 12\mu^2 + 2\mu}{(\Delta^2 + 2\mu)^2}, \quad (2)$$

where $\Delta = \langle N_p \rangle - \langle N_{\bar{p}} \rangle$ is the average number of net-protons, and $\mu = (\langle N_p \rangle + \langle N_{\bar{p}} \rangle) / 2$ is the mean value of protons and antiprotons in the event sample. More details of the calculation of this formula could be found in the appendix.

In Fig. 1 (a) and (b), we show the results of B_3 and B_4 as a function of number of participants (N_{part}) from AMPT default (solid circle), AMPT with string melting (open circle), and THERMINATOR (open square) models in Au + Au collisions at $\sqrt{s_{NN}} = 200$ GeV, respectively. For comparison, the statistical fluctuations of the Binder ratios, calculated from Eq. (2), are presented as dashed lines. We can see that in both transport and statistical models, the statistical fluctuations give main contributions to the Binder ratios. It shows that the influence of statistical fluctuations are not negligible in the measurement of net-proton Binder ratios at RHIC energy.

III. DYNAMICAL NET-PROTON BINDER RATIOS

In the THERMINATOR model, it is well-known that the fluctuations are thermal. From Fig. 1, we observe it gives a good agreement with the Skellam statistical fluctuations. It is difficult to disentangle purely statistical effects from thermal fluctuations which follow the physics of a hadron resonance gas. Since neither of them is associate with the QCP behavior, we suggest to eliminate these statistical or thermal fluctuations in order to get the dynamical part.

As shown in section II, the statistical fluctuations of Binder ratio can be expressed by Eq. (2) given proton

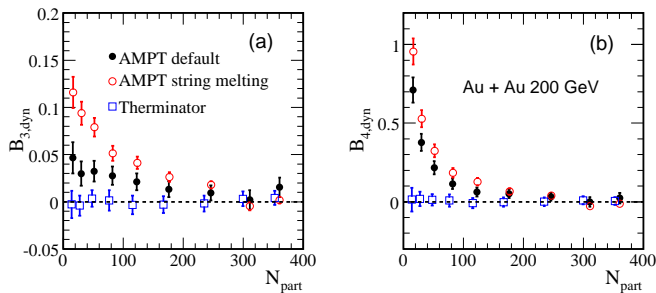


FIG. 2: The third (a) and forth (b) order dynamical Binder ratios as a function of N_{part} from AMPT default (solid circle), AMPT with string melting (open circle), and THERMINATOR (open square) models in Au + Au collisions at $\sqrt{s_{NN}} = 200$ GeV.

and antiproton obey independent Poisson distributions. We define the so-called dynamical Binder ratios as,

$$\begin{aligned} B_{3,dyn} &= B_3 - B_{3,stat} \\ B_{4,dyn} &= B_4 - B_{4,stat}. \end{aligned} \quad (3)$$

We suggest to measure these dynamical Binder ratios instead of the original definition given by Eq. (1) in relativistic heavy ion experiment.

The dynamical net-proton B_3 and B_4 as a function of N_{part} from AMPT default (solid circle), AMPT with string melting (open circle), and THERMINATOR (open square) in Au + Au collisions at $\sqrt{s_{NN}} = 200$ GeV are shown in Fig. 2 (a) and (b), respectively. We find that both the third and forth order Binder ratios from THERMINATOR are zero at all centralities. This is because that THERMINATOR is based on the hadron resonance gas model and the produced net-protons in the final state obey the Skellam distribution [27]. While, in transport models, both dynamical B_3 and B_4 are larger than zero in peripheral collisions, then tend to be zero in central collisions. The results from AMPT string melting are larger than that from the default model. This is due to different mechanisms of hadronization scheme used for finite state particles in different versions of AMPT models.

IV. ENERGY DEPENDENCE OF DYNAMICAL BINDER RATIOS IN TRANSPORT MODELS

In the upper panels of Fig. 3 (a) and (b), we show the energy dependence of the dynamical B_3 and B_4 at six RHIC energies, 7.7, 9.2, 11.5, 39, 62.4, and 200 GeV from AMPT default model. The nine different symbols represent nine collision sizes (denoted by centralities in experiments). In all beam energies, when centrality goes from most peripheral (70-80% central) to most central (0-5% central) collisions, the dynamical Binder ratios decrease and are close to zero in the most central collisions. It means that both dynamical B_3 and B_4 are system size dependent. From 7.7 GeV to 200 GeV, we observe

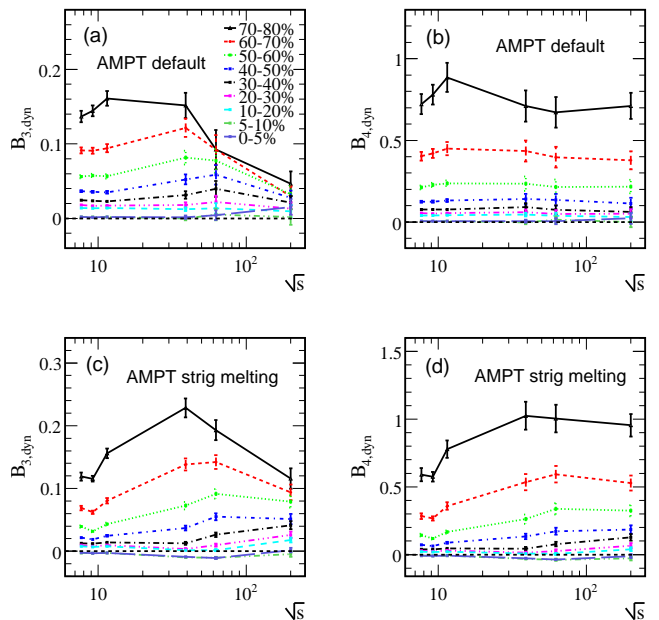


FIG. 3: Energy dependence of the dynamical B_3 (left panel) and B_4 (right panel) at RHIC energies from AMPT default model (upper panel) and string melting (lower panel), respectively. The nine different symbols represent nine collision sizes, which goes from most peripheral (70-80% central) to most central (0-5% central) collisions. The lines are used only to guide eyes.

no platform from the AMPT default model. The lower panels of (c) and (d) for the string melting version give similar results.

Therefore, there is no step function behavior observed in both two versions of the AMPT models. This is understandable since there is no QCD critical mechanism implemented in these transport models.

V. SUMMARY AND OUTLOOK

In this paper, the statistical and dynamical Binder ratios of net-proton are studies in Au + Au collisions at RHIC energies. Using transport and statistical models, it is shown that statistical fluctuations are not negligible in the measurement of higher Binder ratios in relativistic heavy ion collisions.

In order to obtain a clean signature which may be related to the critical point, we suggest to use the dynamical Binder ratio in experimental measurement. The dynamical net-proton Binder ratio is found to be zero in the THERMINATOR model but larger than zero in peripheral collisions in AMPT model. The energy dependence of dynamical Binder ratios with different system sizes shows no step function behavior either in AMPT default or string melting models.

Whether the critical behavior of 3D-Ising model without external field suggested in ref. [15] correspond to the QCD critical point could be discussed. Future work on

the study of projecting the QCD parameters onto the ones in the Ising model and find a path in the phase diagram that corresponds to the vanishing external field are needed. The alternative way is that one can include the external field into the Ising model and then relate it to the Binder ratios to explore the QCD critical point. F. Karsch et al have explored this way in the 3-state Potts model [28]. The analysis in the O(N) models including the 3D-Ising model is thus called for.

It is interesting to investigate the behavior of the dynamical Binder ratios in the coming high energy collisions at RHIC, SPS, and FAIR experiments, where the critical incident energy of QCD phase transition may be covered. Our model study can serve as a background study of the behavior expected from known physics effects for the experimental search for the QCD critical point.

VI. ACKNOWLEDGMENTS

We thank Dr. Lizhu Chen and Shusu Shi for valuable discussions and remarks. This work is supported in part by the NSFC of China with project No. 11005046 and No. 10835005.

VII. APPENDIX: BINDER RATIOS FROM SKELLAM DISTRIBUTION

Given the distributions of proton and antiproton are independent Poisson distributions with mean values are $\langle N_p \rangle$ and $\langle N_{\bar{p}} \rangle$, the net-proton will follow a Skellam distribution. If we define the net-proton as $M = N_p - N_{\bar{p}}$,

then the probability distribution function of M is

$$f(M; \langle N_p \rangle, \langle N_{\bar{p}} \rangle) = e^{-(\langle N_p \rangle + \langle N_{\bar{p}} \rangle)} \left(\frac{\langle N_p \rangle}{\langle N_{\bar{p}} \rangle} \right)^{M/2} I_{|M|} \left(2\sqrt{\langle N_p \rangle \langle N_{\bar{p}} \rangle} \right),$$

where $I_{|M|} \left(2\sqrt{\langle N_p \rangle \langle N_{\bar{p}} \rangle} \right)$ is the modified Bessel function of the first kind.

The n^{th} moment of M , which is defined as $\langle M^n \rangle = \int_{-\infty}^{\infty} M^n f(M; \langle N_p \rangle, \langle N_{\bar{p}} \rangle) dM$, can be calculated from the above distribution function. We obtain

$$\begin{aligned} \langle M \rangle &= \Delta \\ \langle M^2 \rangle &= \Delta^2 + 2\mu \\ \langle M^3 \rangle &= \Delta^3 + 6\mu\Delta + \Delta \\ \langle M^4 \rangle &= \Delta^4 + 12\mu\Delta^2 + 4\Delta^2 + 12\mu^2 + 2\mu, \end{aligned}$$

where $\Delta = \langle N_p \rangle - \langle N_{\bar{p}} \rangle$ is the average number of net-protons, and $\mu = (\langle N_p \rangle + \langle N_{\bar{p}} \rangle) / 2$ is the mean value of proton and antiproton.

By the definitions of the third and forth Binder ratios of Eq. (1), we get the Binder ratios of the Skellam statistical distribution as

$$\begin{aligned} B_{3,stat} &= \frac{\langle M^3 \rangle}{\langle M^2 \rangle^{3/2}} = \frac{\Delta^3 + 6\mu\Delta + \Delta}{(\Delta^2 + 2\mu)^{3/2}}, \\ B_{4,stat} &= \frac{\langle M^4 \rangle}{\langle M^2 \rangle^2} = \frac{\Delta^4 + 12\mu\Delta^2 + 4\Delta^2 + 12\mu^2 + 2\mu}{(\Delta^2 + 2\mu)^2}. \end{aligned}$$

-
- [1] J. Adams *et al.*, Nucl. Phys. **A 757**, 102 (2005).
 - [2] Y. Aoki *et al.*, Nature **443**, 675 (2006).
 - [3] Y. Aoki *et al.*, Phys. Lett. **B 643**, 46 (2006); M. Cheng *et al.*, Phys. Rev. **D 74**, 054507 (2006).
 - [4] E.S. Bowman and J.I. Kapusta, Phys. Rev. **C 79**, 015202 (2009); S. Ejiri, Phys. Rev. **D 78**, 074507 (2008).
 - [5] M.A. Stephanov, Prog. Theor. Phys. Suppl. **153**, 139 (2004); Z. Fodor and S.D. Katz, JHEP **0404**, 50 (2004).
 - [6] R.V. Gavai and S. Gupta, Phys. Rev. **D 78**, 114503 (2008); Phys. Rev. **D 71**, 114014 (2005).
 - [7] B. Mohanty, Nucl. Phys. **A 830**, 899c (2009).
 - [8] B.I. Abelev *et al.*, Phys. Rev. **C 81**, 024911 (2010); STAR internal Note - SN0493 (2009).
 - [9] V. Koch, *et al.* Phys. Rev. Lett. **95**, 182301 (2005); M. Asakawa, *et al.* Phys. Rev. Lett. **85**, 2072 (2000).
 - [10] M. Asakawa, U.W. Heinz, and B. Muller, Phys. Rev. Lett. **85**, 2072 (2000); S. Jeon and V. Koch, Phys. Rev. Lett. **85**, 2076 (2000).
 - [11] M.A. Stephanov, K. Rajagopal, and E.V. Shuryak, Phys. Rev. Lett. **81**, 4816 (1998); Y. Hatta and T. Ikeda, Phys. Rev. **D 67**, 014028 (2003).
 - [12] J. Kapusta, arXiv:1005.0860; D. Bower and S. Gavin, Phys. Rev. **C 64**, 051902 (2001).
 - [13] Y. Hatta and A. Stephanov, Phys. Rev. Lett. **91**, 102003 (2003); M. Asakawa, *Baryon Number Cumulants and Proton Number Cumulants in Relativistic Heavy Ion Collisions*, talks given in the 7th International workshop on critical point and onset of deconfinement (CPOD2011), Nov. 2011, Wuhan, China.
 - [14] M.M. Aggarwal *et al.* (STAR Coll.), Phys. Rev. Lett. **105**, 022302 (2010).
 - [15] Lizhu Chen *et al.*, arXiv:1010.1166.
 - [16] K. Binder, Rep. Prog. Phys. **60**, 487 (1997); K. Binder, Z. Phys. **B 43**, 119 (1981).
 - [17] K. Kanaya and S. Kaya, Phys. Rev. **D 51**, 2404 (1995).
 - [18] M.A. Stephanov, Phys. Rev. Lett. **102**, 032301 (2009); M. Asakawa, S. Ejiri, and M. Kitazawa, Phys. Rev. Lett. **103**, 026301 (2009).
 - [19] J. Garca, and J.A. Gonzalo, Physica **A 326**, 464 (2003); P. Forcrand, and O. Philipsen, Phys. Rev. Lett. **105**, 152001 (2010); M. Asakawa, J Phys. **G 36** 064042 (2009).
 - [20] J. Berges, K. Rajagopal, Nucl. Phys. **B 538** 215 (1999).
 - [21] M.A. Halasz *et al.*, Phys. Rev. **D 58** 096007 (1998).
 - [22] C. Athanasiou, K. Rajagopal, and M. Stephanov, Phys. Rev. **D 82**, 074008 (2010); A. Bialas and R. Peschanski, Nucl. Phys. **B 273**, 703 (1986); A. Bialas and R. Peschanski, Phys. Lett. **B 207**, 59 (1988).
 - [23] Z.W. Lin, C.M. Ko, B.A. Li *et al.*, Phys. Rev. **C 72**,

- 064901 (2005).
- [24] A. Kisiel *et al.*, Comput. Phys. Commun. **174**, 559 (2006).
 - [25] C. Pruneau, S. Gavin, S. Voloshin, Phys. Rev. **C 66**, 044904 (2002); STAR Coll., Phys. Rev. **C 79**, 024906 (2009).
 - [26] J.G. Skellam, Journal of the Royal Statistical Society **109**, 296 (1946); X.F. Luo, B. Mohanty, H.G. Ritter, N. Xu, J. Phys. **G 37**, 094061 (2010).
 - [27] P. Braun-Munizinger *et al.*, arXiv:1107.4267.
 - [28] F. Karsch, and S. Sticksan, Phys. Letts. **B 488**, 319 (2000); F. Karsch, Ch. Schmidt, and S. Sticksan, Comput. Phys. Commun. **147**, 451 (2002).